

# Kerr-effect-induced passive $Q$ switching of a monolithic semiconductor diode laser

Michael B. Flynn,\* Liam O'Faolain, and Thomas F. Krauss

School of Physics and Astronomy, University of St Andrews, North Haugh, St Andrews, Fife KY16 9SS, United Kingdom

Received June 29, 2004; revised manuscript received October 17, 2004; accepted December 1, 2004

We present a novel (to our knowledge) method to passively  $Q$  switch monolithic semiconductor diode lasers using a Bragg reflector filled with a polymer exhibiting the Kerr effect. We present numerical modeling of such devices that display  $Q$  switching. We numerically characterize the pulsed laser output in terms of repetition frequency, pulse power, and pulse energy. We also examine the influence of spontaneous emission strength on pulse dynamics. Advantages of this technique include higher repetition rates and very short pulses. © 2005 Optical Society of America

OCIS codes: 140.3540, 190.3270, 230.1480, 130.5990.

## 1. INTRODUCTION

$Q$  switching<sup>1</sup> is a convenient and simple method for obtaining picosecond pulses. A cavity that is in a high loss state and hence a low  $Q$  state will build up a large population inversion owing to pumping. If the  $Q$  is then switched to a high value, the energy in the cavity is emitted as a short optical pulse. This  $Q$  switching may be done actively<sup>2</sup> through electro-optical or acousto-optical methods or even through rotation of the cavity mirrors. Alternatively, one may perform this passively by using a saturable absorber<sup>3</sup> or dispersive  $Q$  switching.<sup>4,5</sup>

We propose a new passive  $Q$ -switching technique using a Bragg mirror<sup>6</sup> with an intensity-dependent reflectivity spectrum. This can be achieved through fabrication of a multilayer mirror structure from materials with a high Kerr coefficient, such as a suitable polymer. The mirror can be filled with the polymer by use of an embossing technique, whereby a thick layer of polymer is spun onto the sample and pressure and heat are applied to force the polymer into the etched features. A diagram of such a mirror is displayed in Fig. 1, and a scanning electron microscope image of a fabricated mirror is given in Fig. 2. An incident pulse will cause the refractive index of the multilayers to change owing to the Kerr effect, thereby shifting the reflectivity spectra. By careful design of the mirror we allow the cavity loss to change from being very high for low intensity within the cavity to much less for more-intense cavity light.

## 2. MIRROR DESIGN

A Bragg mirror consists of a multilayer stack of alternating high and low refractive index materials. By combining the correct refractive index ratios with the correct layer thickness, exceptionally high reflection is obtainable over a range of wavelengths. It is possible to make the multilayer stacks from materials that exhibit the Kerr effect, as already explained. The Kerr effect is a phenomenon that causes a change in a material's refractive index

owing to third order nonlinearity experienced due to the incident light upon it. The refractive index of a Kerr medium is given by

$$n = n_0 + n_2 I, \quad (1)$$

where  $n_0$  is the refractive index in the absence of light,  $n_2$  is the Kerr coefficient, and  $I$  is the intensity of the incident light.

There are several different polymers that could be selected, e.g., polycarbonate ( $n_2 = -2.99 \times 10^{-11} \text{ cm}^2/\text{W}$ ), polydiacetylene ( $n_2 = 3 \times 10^{-8} \text{ cm}^2/\text{W}$ ), and the soluble polymer dialkylaminonitrodiphenylpolyene-DANS, which has a large  $n_2$  value of  $7 \times 10^{-8} \text{ cm}^2/\text{W}$ . For the purposes of this study we select the latter polymer; however, depending on the intended application, it may be necessary to take other factors into account. For example, many polymers suffer from photostability issues and have much shorter lives than would be required for commercial use. In addition, peak polymer absorption may be a problem, depending on the operating wavelength.

We consider a Bragg reflector made from alternating layers of GaAs and air slots filled with the polymer dialkylaminonitrodiphenylpolyene-DANS. GaAs has an  $n_0$  equal to 3.43 with  $n_2$  equal to  $-2.7 \times 10^{-13} \text{ cm}^2/\text{W}$  at  $1.063 \mu\text{m}$ .<sup>7</sup> The polymer has an  $n_0$  equal to 1.62 and a Kerr coefficient of  $7 \times 10^{-8} \text{ cm}^2/\text{W}$ .<sup>8</sup> Sample reflectivity spectra calculated for several incident powers are dis-

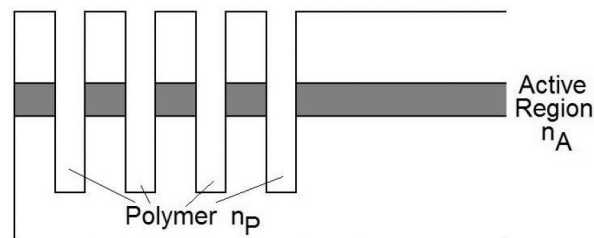


Fig. 1. Diagram of polymer-filled Bragg reflector; the active region has a refractive index of  $n_A$  and the polymer has a refractive index  $n_p$  for no incident light.

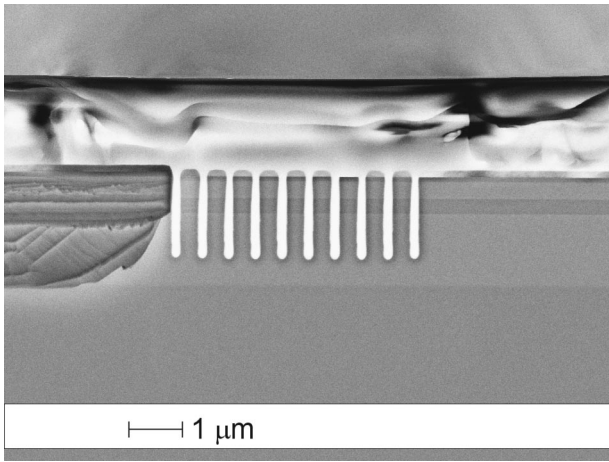


Fig. 2. Scanning electron microscope image of a polymer-filled Bragg reflector. The polymer (shown in white) clearly fills the etched features. The active region is also clearly visible.

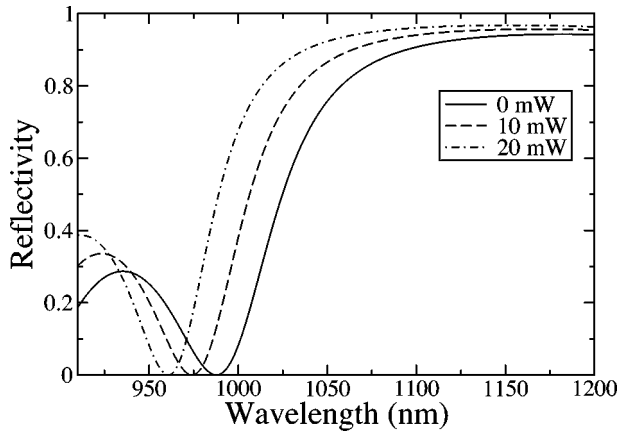


Fig. 3. Reflectivity spectra for Bragg reflector described in text for several different incident powers.

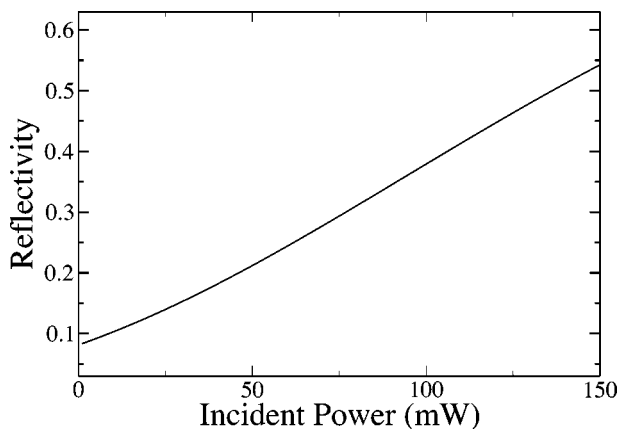


Fig. 4. Reflectivity for Bragg reflector described in text at a wavelength of  $1 \mu\text{m}$  versus incident power.

played in Fig. 3 for a mirror with three periods of 260 nm of GaAs followed by 200 nm of the polymer. To produce the largest reflectivity change at the lasing wavelength one must operate at the band edge of the polymer filled mirror. Figure 4 displays the calculated reflectivity of

the mirror described at a wavelength of  $1 \mu\text{m}$  for incident power in the range of 0–150 mW. All reflectivities were calculated with a transfer matrix method in which the intensity in each layer was used to determine that layer's parameters in a self-consistent manner.

So that the lasing wavelength does not shift, it is essential that the mirrors on either end of the laser are asymmetric around the peak gain. Also, they should be designed such that they experience the same magnitude of wavelength shift for light intensity but in opposite directions. This prevents the lasing wavelength from shifting. We assume that this is the case for our laser cavity. Bragg reflectors can be fabricated to a tolerance of  $\sim 5 \text{ nm}$ ; this may not be sufficient in order to achieve the required asymmetry. However, it should be possible to tune the stop band of the mirror to the correct position with respect to the lasing wavelength by temperature variation.<sup>9</sup>

### 3. NUMERICAL MODEL

We use the following lumped model to link the carrier number  $N$ , the photon number  $S$ , and the gain  $g$  of the semiconductor diode laser:

$$\frac{dN}{dt} = \frac{I}{e} - gS - \frac{N}{\tau_n}, \quad (2)$$

$$\frac{dS}{dt} = (g - g_{\text{th}})S + \beta \frac{N}{\tau_n}, \quad (3)$$

$$g = \frac{\Gamma}{V} g_n (N - N_0), \quad (4)$$

where  $\Gamma = 0.2$  is the confinement factor,  $V = 75 \mu\text{m}^3$  is the active region volume,  $g_n = 2.75 \times 10^{-12} \text{ m}^3 \text{ s}^{-1}$  is the differential gain, and  $N_0 = 1.89 \times 10^8$  is the transparency carrier number, for an injection current  $I$ , an electron charge  $e$ , a carrier lifetime of  $\tau_n = 2.79 \times 10^{-9} \text{ s}$ , and  $\beta = 10^{-5}$  the ratio of the spontaneous emission that is coupled into the lasing mode. The gain threshold  $g_{\text{th}}$  is equal to the cavity loss and is given by

$$g_{\text{th}} = \frac{c}{n_r} \left[ \alpha_{\text{int}} + \frac{1}{2L} \log \left( \frac{1}{R_f R_b} \right) \right], \quad (5)$$

where  $\alpha_{\text{int}} = 25 \text{ cm}^{-1}$  is the dissipative material loss,  $L$  is the length of the laser, and  $R_f$  and  $R_b$  are the reflectivity of the front and back facets, respectively. It is linked to the cavity  $Q$  factor by

$$Q = 2\pi\nu\tau_p, \quad (6)$$

where  $\tau_p = 1/g_{\text{th}}$  is the cavity photon lifetime. The output power from the front facet of the laser is calculated from

$$P(t) = \frac{h\nu c}{2n_r L} \frac{(1 - R_f) \log(1/R_f R_b)}{(1 - \sqrt{R_f R_b})(1 + \sqrt{R_f/R_b})} S(t), \quad (7)$$

where  $h\nu$  is the energy of the emitted photons. The irradiation density is calculated by assuming a waveguide cross-sectional area of  $5 \mu\text{m} \times 0.2 \mu\text{m}$ . The resultant instantaneous mirror reflectivity can then be determined from Fig. 4. The parameter values and model are similar

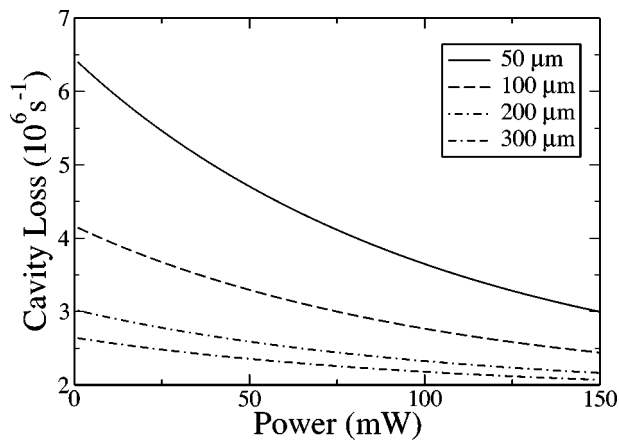


Fig. 5. Cavity loss for several different cavity lengths versus incident power at a wavelength of  $1 \mu\text{m}$ .

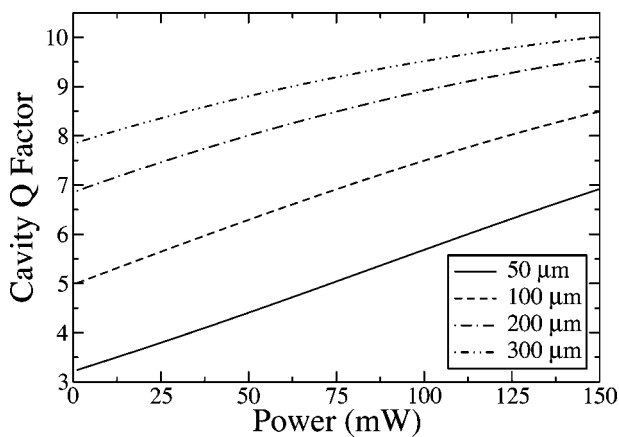


Fig. 6. Cavity Q factor for several different cavity lengths versus incident power at a wavelength of  $1 \mu\text{m}$ .

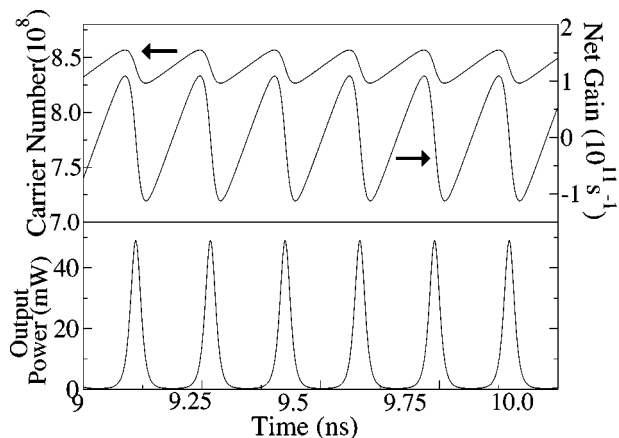


Fig. 7. Plot of optical output, net cavity gain, and carrier number for an injection current of  $I = 100 \text{ mA}$ .

to that used by Ahmed *et al.*<sup>10</sup> The model was solved with a fourth-order Runge–Kutta method.

Figures 5 and 6 display the calculated cavity loss and cavity Q factor, respectively, for several different cavity lengths based on the reflectivity versus power curve in Fig. 4. As is expected, shorter cavities experience a much

larger Q change, owing to facet reflectivity's being a more significant term in the cavity loss. The Q-switching mechanism is clearly evident in the simulation results displayed in Fig. 7.

#### 4. RESULTS

Pulse durations of the order of 5 ps were obtained from the model, which is comparable with the shortest pulses from other methods of Q switching.<sup>1</sup> Higher currents lead to longer pulses (see Fig. 8) as the gain takes longer to deplete, owing to a higher rate of carrier injection. For the shortest optical pulses, the population inversion should be maximized, and the photon lifetime should be minimized.

The repetition rates of passively Q-switched diode lasers incorporating saturable absorbers have been measured up to  $\sim 18.5 \text{ GHz}$  with two gain sections and an absorber<sup>1</sup>; however, typical Q-switching repetition rates extend up to  $\sim 5 \text{ GHz}$ . Figure 8 displays the repetition rate versus current showing high frequency pulsing in the 6–9 GHz range from our simulations. The repetition rate of the pulses is determined by the time taken for the gain to exceed the loss from its fully depleted value, which in turn is related to the carrier density. Unsurprisingly, one of the key factors in the determination of the repetition rate is the pumping current—essentially, the rate at which carriers are increased and build up the gain during the low Q state. The use of the Kerr effect allows for high repetition rates owing to the characteristic time of the Kerr effect on the order of 1 fs, whereas for saturable absorbers the gain finite relaxation time occurs on a time scale of picoseconds, leading to a change in the Q of the cavity of an order of magnitude faster than the pulse durations in the case of the Kerr effect.

Figure 9 shows the output peak powers of the pulses versus the pumping current. This yields a strong linear relationship with the pumping current. Our model did not include nonlinear effects such as gain compression, and therefore the linear relationship is valid only over a specific range of currents in a practical device.

The influence of spontaneous emission on the laser dynamics is important and can be seen from Eqs. (2) and (3), which form a stiff system owing to the differing time con-

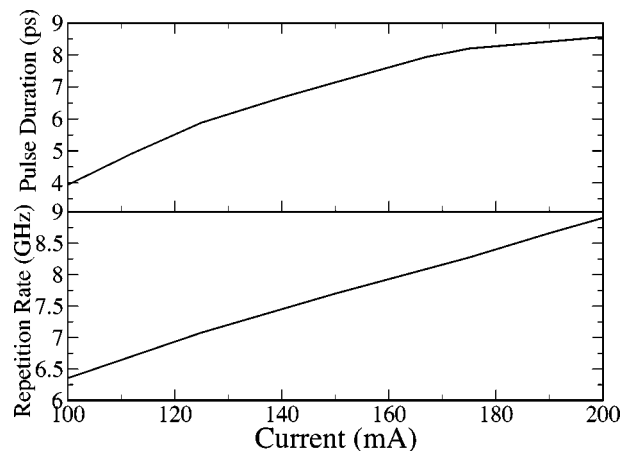


Fig. 8. Plot of pulse duration and repetition rate for  $50\text{-}\mu\text{m}$ -long device versus current.

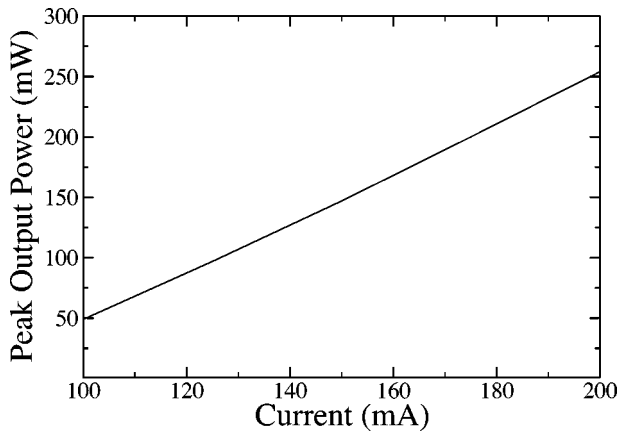


Fig. 9. Plot of peak output power for 50- $\mu\text{m}$ -long device versus current.

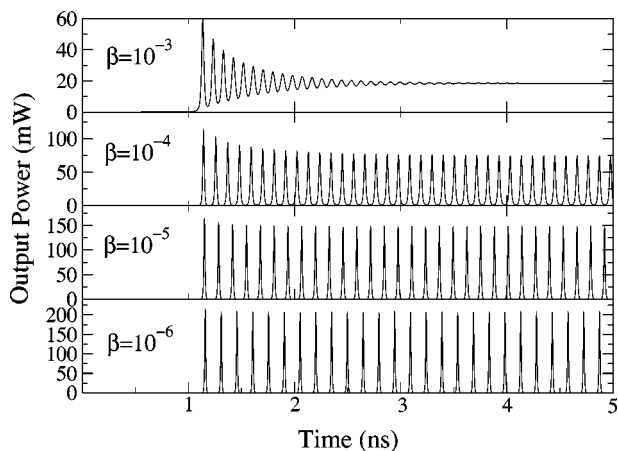


Fig. 10. Effect of spontaneous emission factor on  $Q$ -switching dynamics for an injection current of  $I = 150$  mA.

stants. In this system the  $\beta$  parameter acts as a damping factor. Figure 10 displays the output power as a function of time for an injection current of 150 mA and a range of spontaneous emission factors. An increase in  $\beta$  inhibits  $Q$ -switching behavior and leads to reduced peak power output, increased repetition rate, and longer pulse durations owing to the spontaneous emission changing the relationship between cavity gain and loss.

## 5. CONCLUSION

We have described a new technique for passively  $Q$ -switching semiconductor diode lasers that involves incorporating a Kerr medium into a Bragg reflector. This leads to a multilayer mirror whose reflectivity spectra

shift in wavelength with incident power. We have suggested suitable materials and dimensions for the construction of an actual device based on numerical modeling. Although standard fabrication tolerances are not sufficiently high to construct Bragg mirrors to the correct accuracy, one can use temperature tuning to shift the Bragg reflectivity spectra to the correct wavelength. This method is very suitable for exceptionally short cavities of the order of tens of micrometers, which is not possible with saturable absorber  $Q$  switching or dispersive  $Q$  switching.<sup>4</sup> We have numerically characterized expected device operation and performance in terms of repetition frequency, pulse duration, and pulse energy. We have also discussed the effect of spontaneous emission on the laser  $Q$ -switching dynamics. These results have showed the possibility of producing high peak power, high-frequency pulses of approximately 5-ps duration.

\*M. B. Flynn's e-mail address is mbf@st-and.ac.uk.

## REFERENCES

1. P. P. Vasil'ev, I. H. White, and J. Gowar, "Fast phenomena in semiconductor lasers," *Rep. Prog. Phys.* **63**, 1997–2042 (2000).
2. A. E. Siegman, *Lasers* (University Science, Mill Valley, Calif., 1986).
3. C. Harder, K. Y. Lau, and A. Yariv, "Bistability and pulsations in semiconductor lasers with inhomogeneous current injection," *IEEE J. Quantum Electron.* **6**, 1351–1361 (1982).
4. B. Sartorius, M. Möhrle, S. Reichenbacher, H. Preier, H. Wünsche, and U. Bandelow, "Dispersive self- $Q$ -switching in self-pulsating DFB lasers," *IEEE J. Quantum Electron.* **33**, 211–218 (1997).
5. U. Bandelow, H. Wünsche, B. Sartorius, and M. Möhrle, "Dispersive self- $Q$ -switching in DFB lasers: theory versus experiment," *IEEE J. Sel. Top. Quantum Electron.* **3**, 270–278 (1997).
6. R. Jambunathan and J. Singh, "Design studies for distributed Bragg reflectors for short-cavity edge-emitting lasers," *IEEE J. Quantum Electron.* **33**, 1180–1189 (1997).
7. A. A. Said, M. Sheik-Bahae, D. J. Hagan, T. H. Wei, J. Wang, J. Young, and E. W. Van Stryland, "Determination of bound-electronic and free-carrier nonlinearities in ZnSe, GaAs, CdTe, and ZnTe," *J. Opt. Soc. Am. B* **9**, 405–414 (1992).
8. M. B. Marques, G. Assanto, G. I. Stegeman, G. R. Mohlmann, E. W. P. Erdhuisen, and W. H. G. Horsthuis, "Large nonresonant intensity dependent refractive index of 4-dialkylamino-4'-nitro-diphenyl-polyene side chain polymers in waveguides," *Appl. Phys. Lett.* **94**, 756–763 (2003).
9. J. L. Shen, C. Y. Chang, W. C. Chou, M. C. Wu, and Y. F. Chen, "Temperature dependence of the reflectivity in absorbing Bragg reflectors," *Opt. Express* **9**, 287–293 (2001), <http://www.opticsexpress.org/>.
10. M. Ahmed, M. Yamada, and M. Saito, "Numerical modeling of intensity and phase noise in semiconductor lasers," *IEEE J. Quantum Electron.* **37**, 1600–1610 (2001).